

# DIGITAL READOUT TECHNIQUE FOR LARGE ARRAYS OF SUPERCONDUCTING DETECTORS

Interim Report

JPL Task 1056

Inseob Hahn, Science and Technology Development Section (354)  
P. Day, Microwave Experiment Systems & Technology (386)  
H. LeDuc, Microwave Experiment Systems & Technology (386)

## A. OBJECTIVES

The Tropospheric Emission Spectrometer (TES) is widely considered to be the next-generation technology for space-based millimeter, sub-millimeter and x-ray astronomical observations. These sensors are superior to bolometric sensors using neutron transmutation doped (NTD) germanium because of their greater bandwidth and higher operating temperature. In addition, TESs are fabricated using standard lithographic techniques, making them suitable for the large-format focal-plane arrays required for future space telescope missions such as SAFIR, CMB-POL and Constellation-X. An unsolved problem is the readout scheme for large arrays of TESs. Individual sensors are read out using a Superconducting Quantum Interference Device (SQUID), a type of current amplifier that operates at cryogenic temperatures. To keep the number of wires running between the cooled focal plane and the room-temperature electronics manageable, a low-temperature multiplexing scheme must be implemented. One strategy being pursued by a group at NIST is to wire traditional analog direct current (dc) SQUIDs in an array and turn on a common bias current for columns of the array one at a time.[1] The voltage measured on a common voltage lead wired across the array corresponds only to the SQUID in the activated column. However this strategy often faces a challenge associated with crosstalk between lines and the settling time of the feedback circuit.

To overcome these difficulties, we have proposed a new way to achieve the multiplexing readout technique for TES arrays. The main idea is to convert the signal from each pixel of the detector to a digital representation immediately, using the superconducting version of a voltage-to-frequency converter. These devices, called relaxation-oscillation SQUID (ROS), use an inductively-shunted, hysteretic SQUID as a relaxation oscillator, converting a current signal -- from the transition edge sensor in this case -- into a train of pulses at a particular frequency corresponding to the current signal. The signal is reconstructed with a simple counter at room temperature. First-year objectives of the task are to simulate, design, fabricate and test a prototype ROS.

## B. PROGRESS AND RESULTS

### 1. Simulations and design of ROS

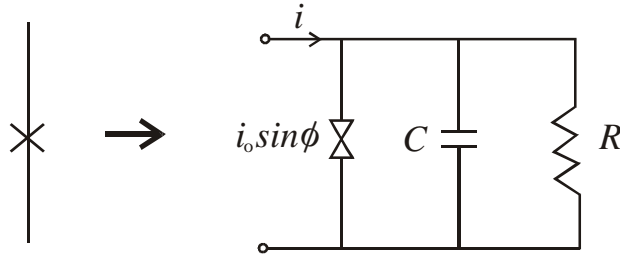


Figure 1 - Junction Model

A single Josephson junction is conveniently modeled by a shunted resistor ( $R$ ) and a capacitor ( $C$ ) together with the junction itself. The junction consists of two superconductors separated by a thin insulating tunneling barrier. The tunneling current through the barrier can be expressed by the dc Josephson relationship,  $I = I_0 \sin \phi$ , where  $I_0$  is the critical current and  $\phi$  is the phase difference across the junction. Figure 1 shows the resistively-shunted-junction (RSJ) model. These are parasitic elements in the SQUID, and are part of the fabrication. In a relaxation oscillation superconducting interference device (ROS), a hysteretic dc SQUID is shunted by a series of a resistor ( $R_{sh}$ ) and an inductor ( $L_{sh}$ ) as shown in the Fig. 2. The basic operation of such a circuit is that initially, the junction is in a superconducting state (zero-voltage stage), and thus shunts all current through the junction. With the critical current is reached, the

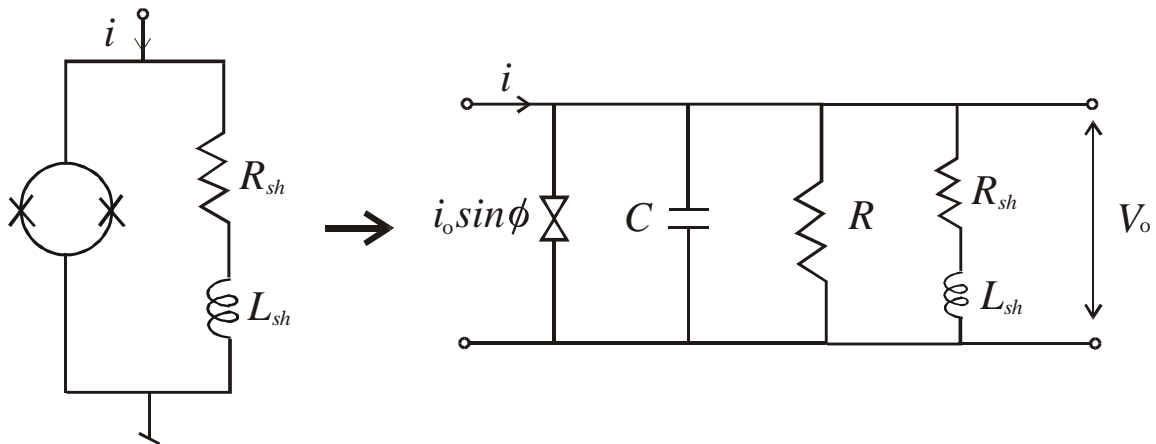


Figure 2 - relaxation oscillation SQUID, single junction approximation

junction becomes no longer superconducting, and a voltage appears across the junction, as well as across the shunt branch. The finite resistance in the junction now allows current to discharge through the shunt  $RL$  circuit. When the current discharges to zero, the initial conditions are met again, and the charging and discharging repeats. During the relaxation oscillation, the voltage across the ROS oscillates between  $V=0$  and  $V \sim V_g$ . Both the frequency and the duty cycle depend on the bias current and on the critical current. The critical current is a function of the flux in the SQUID and, consequently, a ROS can be used as a flux-to-frequency or flux-to-voltage converter. The natural frequency of the ROS can be adjusted by adjusting the shunt resistor and

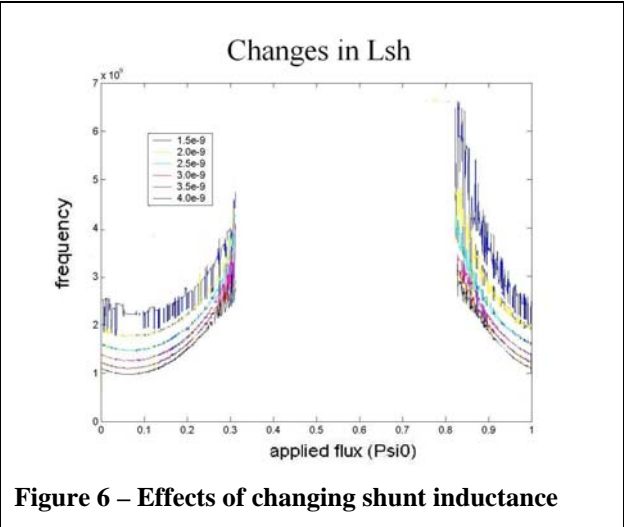
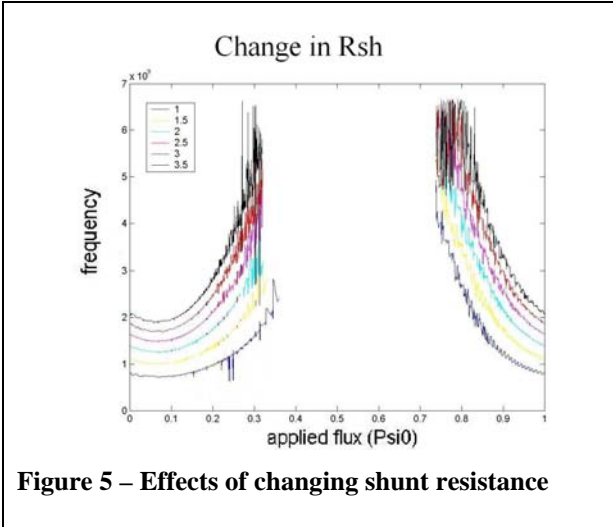
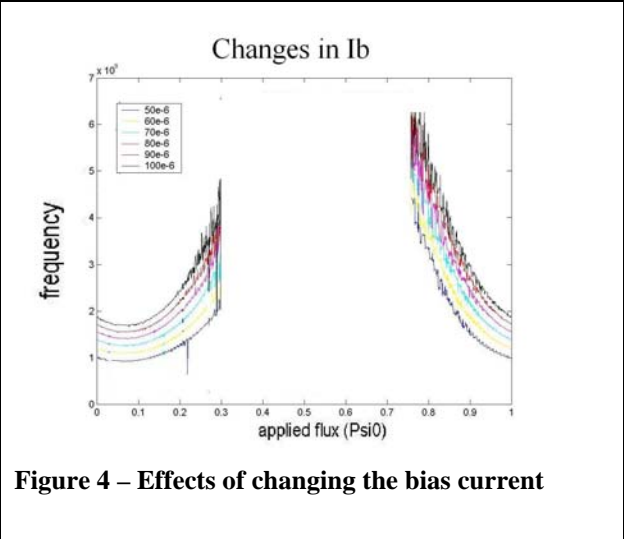
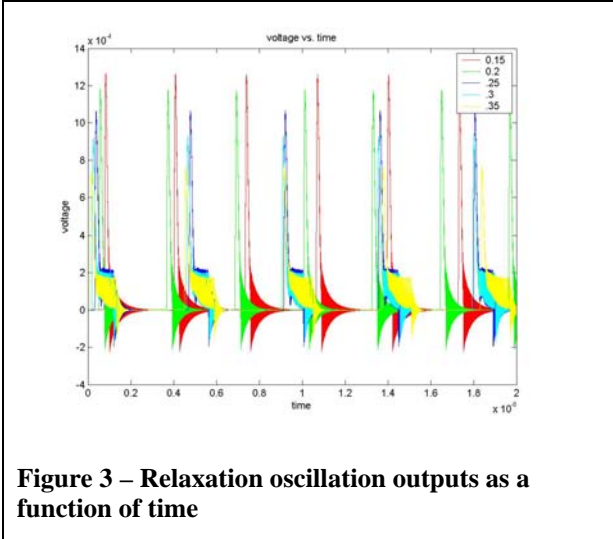
shunt inductor, as the charging and discharging times of the shunt branch determine the period of oscillations. The period can be calculated as  $t_0 = L_s/R_s \ln[1 - I_{max}(\Phi)/I_b]$ . [2] In many analyses, it is convenient to consider the SQUID as a single junction with a critical current controlled by the applied field. In this project, however, we have modeled a ROS with two junctions including the self-inductance of the superconducting for better predictions. Results of time domain simulations are shown in Fig 3. All the units are in MKS. The output voltage is plotted against time, and the different colored curves are for different applied flux quanta through the superconducting loop. As expected, different applied fluxes produce different periods of oscillation. The results of the other simulations are shown in figures 4-8. Figure 4 shows the different bias currents applied to the SQUID circuit. It can be seen that as the bias current increases, the frequency of output is increased for the same applied flux. When the current charges through the SQUID, current is decaying exponentially in the  $RL$  shunt circuit; when the current discharges in the SQUID, the current is charging exponentially and asymptotically to the bias current. By setting the bias current higher, the current charges and discharges faster, thus decreasing the period of oscillations and increasing the frequency.

The next results involve changing the shunt resistance value. As mentioned before, the charging and discharging of the  $RL$  shunt circuit is at an exponential rate. With the voltage nearly constant, both when the Josephson Junction is in the superconducting state ( $V = 0$ ) and when the Josephson Junction is not in the superconducting state ( $V = V_c$ ), we can use the solution for a dc  $RL$  circuit to approximate the behavior of the current as:

$$I = I_b(1 - e^{-\frac{R}{L}t}) \quad \text{charging case}$$

$$I = I_b(e^{-\frac{R}{L}t}) \quad \text{discharging case}$$

The  $L/R$  constant in the exponential is the time constant of the  $RL$  shunt branch. As  $R$  increases, and as  $L$  decreases, the time constant decreases. This would suggest a shorter period of oscillation and a higher frequency. This is the exact trend observed in figures 5 and 6. We also attempt to observe any trends in changing the junction properties of the SQUID. Because these components are in parallel with each other, and are in series with the self-inductance of the SQUID, we would expect nonlinear results when manipulating these parameters. This is in fact what we get, as observed in figures 7 and 8. There is no linear trend of the output frequency against the changing parameters.



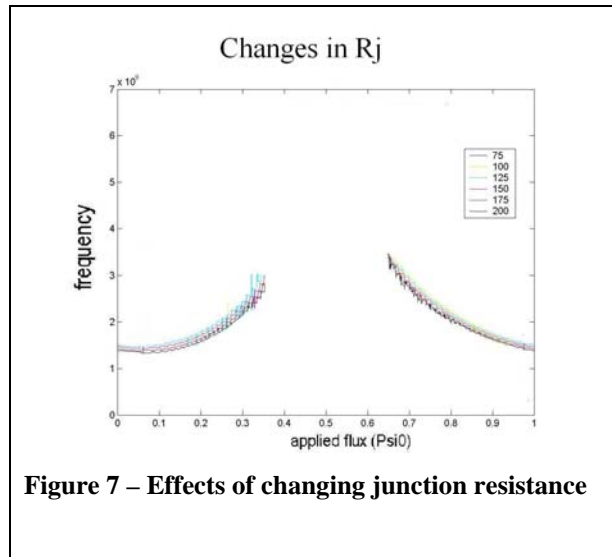


Figure 7 – Effects of changing junction resistance

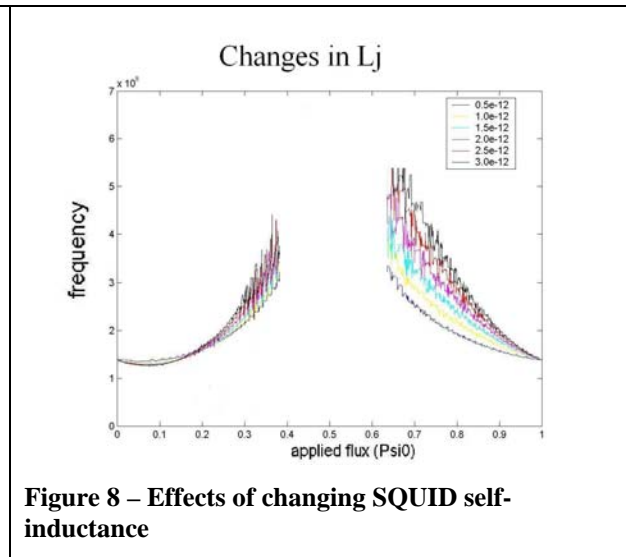


Figure 8 – Effects of changing SQUID self-inductance

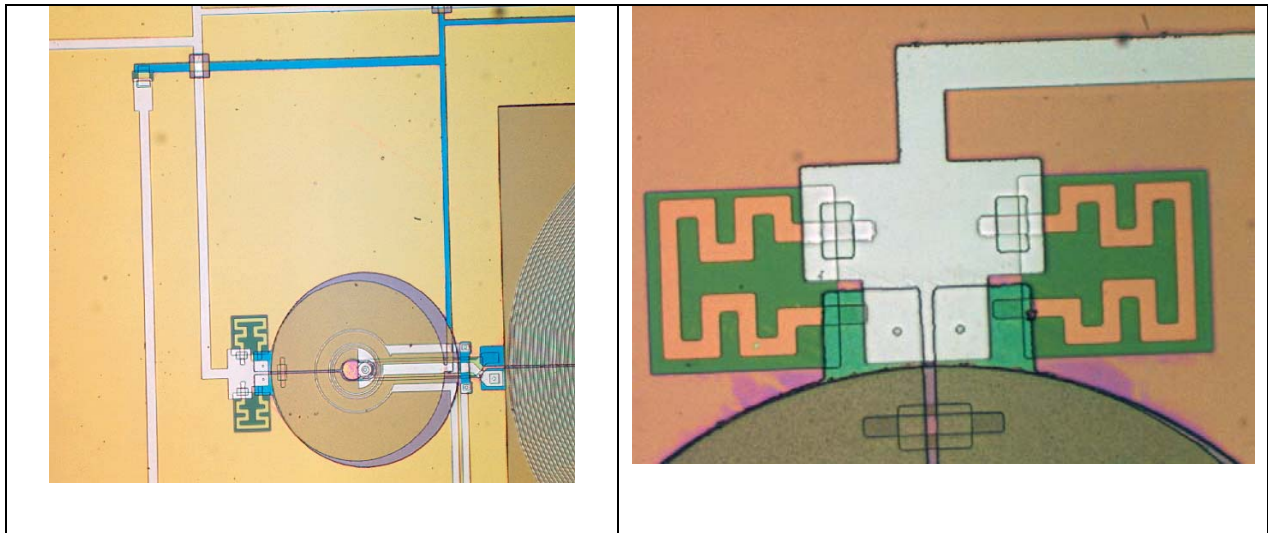
Based on the above numerical simulations of the ROS, we have developed three practical designs for ROSs for thin film fabrications. Table 1 summarizes the current design parameters for three ROSs. To obtain the relaxation oscillation condition, the effective hysteresis parameter  $\beta_c^*$ , defined by  $2\pi I_c R_{sh}^2 C_{sq} / \Phi_0$ , has to be close to unity.

Table1. Design parameter of JPL ROS device

Parameters	ROS_0.5	ROS_1.0	ROS_2.0	Definition
$I_c \times 2$	45	45	45	Critical current junction (microA)
$R_d / 2$	28	28	28	SQUID shunt resistor (Ohm)
$C_j \times 2$	0.8	0.8	0.8	Junction capacitance (pF)
junction width	3	3	3	Micron
$L_{sq}$	25	25	25	SQUID inductance (pH)
$R_{sh}$	2	2	2	Shunt resistor (Ohm)
$L_{sh}$	3.7	2.1	1.0	Shunt inductor (nH)
$a$	900	550	300	Square inductor dim. (Micron)
$b$	10	10	10	Inductor wire dim. (Micron)
$f_0$	0.5	1.0	2.0	Resonance freq. (GHz)
$\beta_c$	90	90	90	Hysteresis parameter
$\beta_c^*$	0.5	0.5	0.5	ROS effective hysteresis parameter.
$\beta_L$	0.6	0.6	0.6	Screening parameter
$I_{n,Rd} (rms)$	9.1E-07	9.1E-07	9.1E-07	Current noise by Rd (A)
$I_{n,Rsh} (rms)$	2.5E-07	3.3E-07	4.9E-07	Current noise by Rsh (A)
$I_{op}$	30.6	30.6	30.6	Optimal bias current (microA)

## 2. Fabrication of ROS

Three different prototypes ROSs have been fabricated using thin films with the aid of photolithography. The dc SQUID design is a typical circular washer style with a circular hole. Its inductance is given by  $L = \mu_0 d$  where  $d$  is the diameter of the hole.[3] The main junction is a trilayer structure Nb/Al-AIO<sub>x</sub>/Nb. The resistor is made by depositing thin films of Pd-Au. The shunt inductor is a single square loop of Nb. The insulation between each layer is SiO<sub>2</sub>. Tunnel junctions, the other Nb structures, were patterned with reactive ion etching. Figure 9 shows a prototype ROS that has been fabricated. We are currently testing the device at helium temperature.



**Figure 9. Photographs of a prototype ROS under test. The junction (two small circular features in the middle of the picture on the right) is 3 μm x 3 μm.**

### **C. SIGNIFICANCE OF RESULTS**

We have designed and fabricated a first-prototype ROS for digital readout of a transition edge sensor. Numerical simulations of the ROS device have been completed.

### **D. FINANCIAL STATUS**

The total funding for this task was \$200,000, of which approximately \$130,000 has been expended.

### **E. PERSONNEL**

Mr. Yiyang Gong, Caltech student, has performed the ROS numerical simulation as a Caltech summer undergraduate research fellowship (SURF) project.

### **F. PUBLICATIONS**

None.

### **G. REFERENCES**

- [1] Carl D. Reintsema, Jörn Beyer, Sae Woo Nam, Steve Deiker, Gene C. Hilton, Kent Irwin, John Martinis, Joel Ullom, and Leila R. Vale, "Prototype system for superconducting quantum interference device multiplexing of large-format transition-edge sensor arrays" *Rev. Sci. Instrum.* 74, 4500 (2003).
- [2] D. J. Adelerhof, H. Nijstad, J. Flokstra and H. Rogalla, "Relaxation oscillation SQUIDs with high flux-to-voltage transfer: Simulations and experiments" *J. Appl. Phys.* 39, 2661 (1994).
- [3] M. B. Ketchen "Integrated thin-film dc SQUID sensors," *IEEE Trans. Magn. MAG-23*, 1650 (1987).